CHEMISTRY
A EUROPEAN JOURNAL

DOI: 10.1002/chem.200902883

Electronic Structure and Reactivity of a [1],[1]Disilamolybdenocenophane

Thomas Arnold, Holger Braunschweig,* Manuela Gross, Martin Kaupp,* Robert Müller, and Krzysztof Radacki[a]

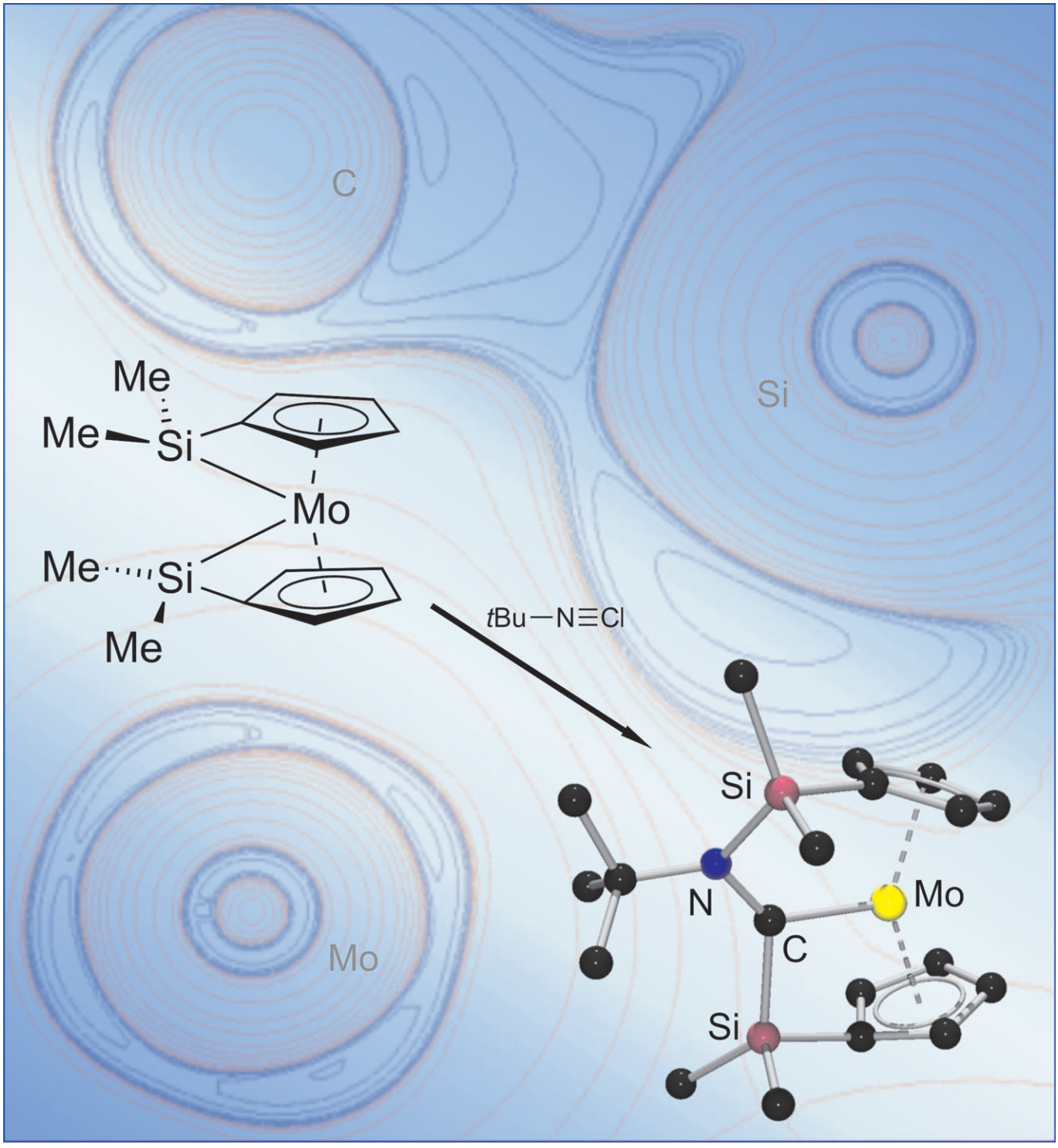

Abstract: The electronic structure of the two-fold bridged [1],[1]disilamolybdenocenophane has been analyzed by means of density functional theory. As predicted, the relatively high charge at the metal center and, in particular, the highly strained geometry determine a noticeable reactivity towards unsaturated organic substrates. Thus, treatment with the nonpolar reagents 2-butyne and azobenzene leads to side-on coordination of the substrate to the metal center, whereas the reaction with polar *tert*-butylisonitrile gives a highly unusual structural motif in the form of an *ansa*-carbene.

Keywords: *ansa*-complexes · density functional calculations · molybdenum · silicon

Introduction

Metallocenophanes have attracted great attention in recent decades due to their applications in catalysis and materials science as precursors for inorganic polymers obtained through ring-opening polymerization (ROP).[1] Therefore, [1]- and [2]metallocenophanes are a focus of research due to their unique structure and reactivity pattern. Up to now, metallocenophanes have been extensively investigated with regard to ligand exchange reactions at the metal center and to haptotropic shifts of the cyclopentadienyl ligands.[1f–h,2] Furthermore, the chemical properties of the bridging moiety have been extensively studied, particularly the insertion of late transition metal fragments into the E–C_{ipso} bond of [1]metallocenophanes, which is considered to be the key step in transition-metal-catalyzed ROP.[1a–e,3] In contrast, [2]metallocenophanes commonly undergo oxidative additions of the E–E bridge to zerovalent late transition metal fragments. Based on the facile activation of the E–E bond, both homogeneously and heterogeneously catalyzed insertions of unsaturated organic substrates into E–E bridges have been observed.[4]

Recently, we succeeded in the first intramolecular insertion of a metal center into the bridging moiety. Treatment of 1,1,2,2-tetramethyl[2]disilamolybdenocenophanedihydride under photolytic conditions led to reductive elimination of hydrogen and a facile oxidative addition of the Si–Si moiety to the molybdenum center (Scheme 1). Thus, two-fold bridged [1],[1]disilametallocenophane **1** was obtained, which contributes an unprecedented structural motif to the class of *ansa*-complexes.[5]

Herein, we report on detailed density functional theory (DFT) studies that reveal the electronic structure of the title compound and additionally on the first results of the unusual reactivity of two-fold bridged *ansa*-complex **1** towards polar and nonpolar unsaturated organic substrates.

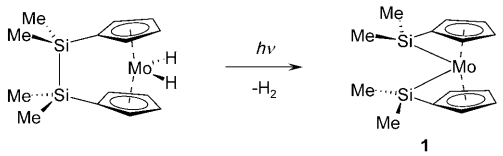

Scheme 1. Synthesis of [1],[1]disilamolybdenocenophane **1**.

Results and Discussion

DFT studies: The bonding situation of mono- and bisfulvene metal complexes, which are to some extent related to the title compound, is described as being between a neutral η^6-coordination (A) and a dianionic η^1:η^5-coordination (B).[6]

To elucidate the electronic structure of **1** in detail and to obtain information as to its potential reactivity, it has been analyzed by means of DFT calculations. Electron localization function (ELF),[7] natural population analysis (NPA),[8] and Bader's topological analysis of the electron density (quantum theory of atoms in molecules, QTAIM[9]) have been employed (for further details see the Supporting Information).

The highest occupied canonical Kohn–Sham MOs of model $\mathbf{1}_{cs}$**, shown in Figure 1, feature a HOMO with predominant molybdenum d_{z^2} character, mixed with smaller contributions from the cyclopentadienyl π systems. This orbital is slightly higher in energy (by $\approx 10\,kJ\,mol^{-1}$) than the HOMO of the corresponding unstrained species [Mo(η^5-C_5H_5)$_2$($SiMe_3$)$_2$] (**2**).

The HOMO–1 and HOMO–2 are symmetrical and unsymmetrical linear combinations, respectively, of the Mo–Si

[a] T. Arnold, Prof. Dr. H. Braunschweig, M. Gross, Prof. Dr. M. Kaupp, R. Müller, Dr. K. Radacki
Institut für Anorganische Chemie
Julius-Maximilians-Universität Würzburg
Am Hubland, 97074 Würzburg (Germany)
Fax: (+49) 931-888-4623
E-mail: h.braunschweig@mail.uni-wuerzburg.de
kaupp@mail.uni-wuerzburg.de

Supporting information for this article is available on the WWW under http://dx.doi.org/10.1002/chem.200902883.

[**] See the Experimental section for model definitions.

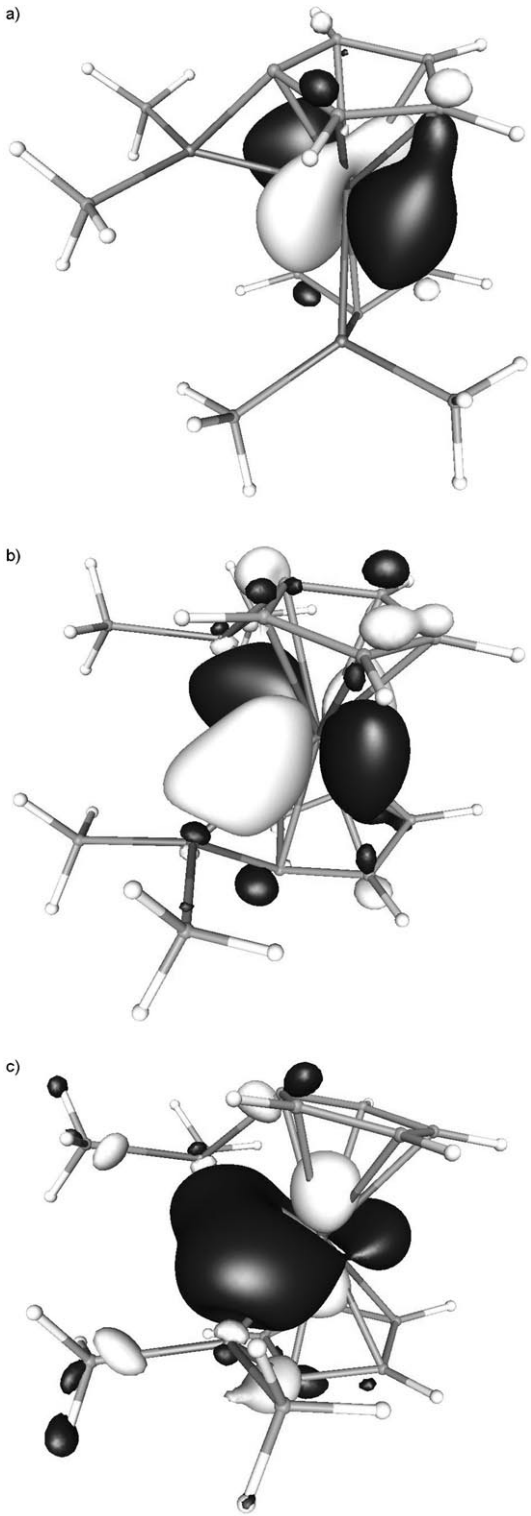

Figure 1. Plots of selected MOs for $\mathbf{1}_{cs}$. a) HOMO, b) HOMO−1, c) HOMO−2.

σ bonds (with participation of molybdenum d_{yz} and $d_{x^2-y^2}$ orbitals). These results are consistent with the known bonding situation for Cp_2ML_n ($n=1$–3) complexes.[10] NPA analyses indicate an appreciable negative charge of −0.50 on Mo. NPA charges at the same computational level for related mono- and bis-silyl-substituted molybdenocene dihydrides range from −0.35 to −0.21, depending on the complex (see the Supporting Information for further details). Together with values of −0.45 for the *ipso* carbon atoms (C_{ipso}), these three centers are identified as most suitable for electrophilic attack. The bridging silicon atoms exhibit NPA charges of about 1.50 and thus mark the higher end of silicon charges (values ranging from 1.43 to 1.24) for the systems under consideration. Wiberg bond indices[11] of 0.61 are consistent with relatively polar Mo−Si bonding and in line with results for related systems.

The direct coordination of the Cp-bound silyl groups to the metal center, consisting of a M-Si-C three-atomic unit, is the most unusual structural motif of **1**. QTAIM analysis for $\mathbf{1}_{cs}$ provides a bond path and a bond critical point (BCP) between silicon and molybdenum (B3LYP/TZVP/12s6p5d data in Figure 2, left; other functionals give the same result).[12]

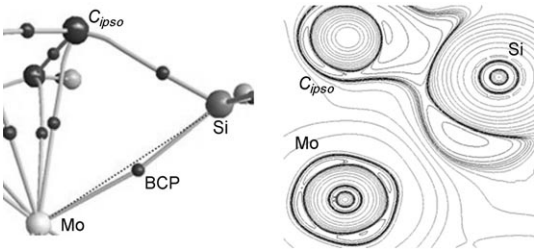

Figure 2. Left: QTAIM-based molecular graph of $\mathbf{1}_{cs}$ showing the Mo-Si-C_{ipso} unit and the slightly bent Mo−Si bond. Bond critical points (BCP) are shown as small dots. Right: Contour plot of the Laplacian in a Mo-Si-C_{ipso} plane of $\mathbf{1}_{cs}$.

The structural parameters of **1**, discussed elsewhere,[5] suggest a highly strained bonding situation. Indeed, the calculated bond paths between the silyl groups and the metal center show a (slightly) convex curvature (Figure 2, left), which is typical for systems exhibiting some ring strain. These results are in agreement with the picture provided by the ELF (Figure 3). Silyl lone-pair-like ELF domains, brought about by the η^1:η^5-coordination mode, point towards the metal center. They are not centered on a straight connection line between silicon and molybdenum but are slightly below. The contour plot of the Laplacian of $\mathbf{1}_{cs}$ provides a similar description (Figure 2, right). The experimentally observed high reactivity of **1** may be, to some extent, a consequence of the release of ring strain. To get a rough estimate of the influence of ring strain on thermochemistry, we considered two comparable reactions consisting of the conversion of **1** and **2** with ethane (Scheme 2). Both (hypothetical) reactions are endothermic, but about 30 kJ mol^{-1} less so in case of the more strained **1**.

The relatively short Mo−Si bonds may indicate some backbonding effects, as discussed for other molybdenum silyl complexes.[13] However, this type of backbonding is difficult to quantify, for example, by the natural bond orbital approach.[14] The bond bending seen in Figure 2, left may

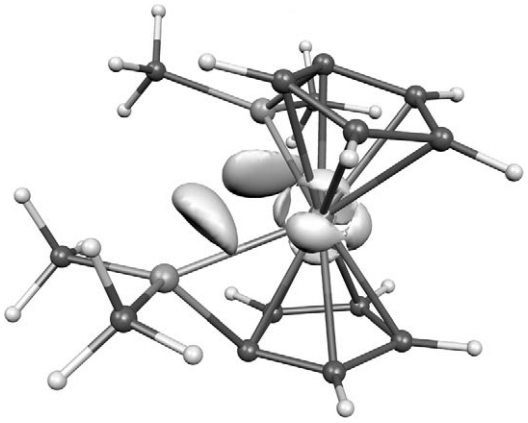

Figure 3. ELF = 0.75 isosurface for $\mathbf{1}_{cs}$. ELF isosurfaces around the Cp rings and silicon methyl groups have been removed for clarity.

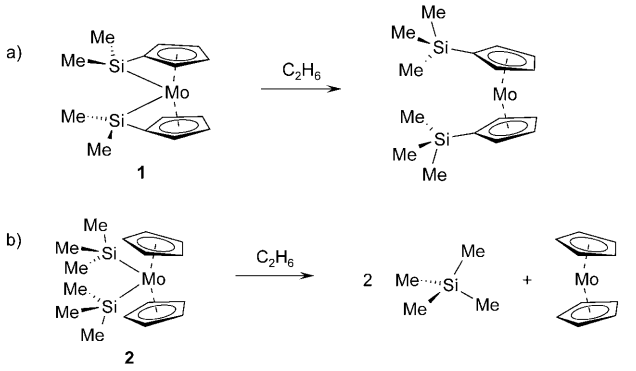

Scheme 2. a,b) Reactions used for estimating the effects of ring strain on thermochemistry. Reaction energies obtained from full structure optimizations at the B3LYP/TZVP level of theory: a) $\Delta E = 37.0\ \mathrm{kJ\,mol^{-1}}$. b) $\Delta E = 66.6\ \mathrm{kJ\,mol^{-1}}$.

also contribute to short bonds as known, for instance, for cyclopropane.[15]

Reactivity studies: Based on the aforementioned computational studies, **1** is predicted to be susceptible to attack at the molybdenum center with cleavage of both Mo–Si bonds. Indeed, treatment of **1** with the unsaturated substrates 2-butyne and *trans*-azobenzene resulted in the clean formation of side-on coordinated alkyne (**3**) and azo complexes (**4**), respectively, with cleavage of the Mo–Si bonds and formation of a Si–Si bridge (Scheme 3). Monitoring the reactions by using ^{1}H NMR spectroscopy revealed the absence of any soluble byproducts, thus indicating quantitative conversion of **1**. Orange complex **3** is slightly air and moisture sensitive, whereas red complex **4** showed no decomposition over several days. Both products were isolated in about 50% yield. Complex **3** appears C_{2v} symmetric in solution as indicated by the ^{1}H NMR spectrum, which displays two virtual triplets for the cyclopentadienyl protons at $\delta = 4.63$ and 3.71 ppm and one singlet at $\delta = 0.39$ ppm for the methyl groups bound to the silicon nuclei. The ^{13}C NMR shift of the quaternary carbon atoms of the butyne ligand at $\delta = 114.6$ ppm is typical

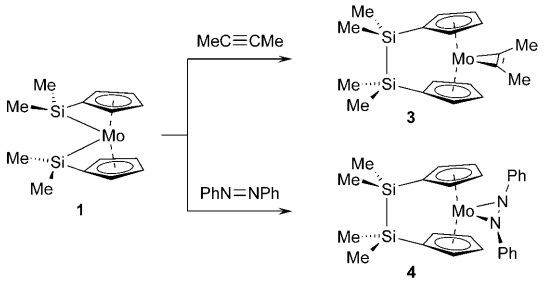

Scheme 3. Reactivity of **1** towards nonpolar unsaturated organic substrates.

for side-on coordinated "two-electron" alkynes, such as the pertinent ^{13}C NMR shift of the nonbridged derivative [Mo(η^5-C_5H_5)$_2$(η^2-MeCCMe)] at $\delta = 114.8$ ppm.[16] As imposed by the mutual *trans* position of the phenyl groups bound to nitrogen, **4** appears only C_2 symmetric in solution. In the ^{1}H NMR spectrum, four signals can be detected for the cyclopentadienyl protons at $\delta = 5.09$, 4.82, 4.63 and 3.92 ppm and two signals for the silicon-bound methyl protons at $\delta =$ 0.17 and 0.10 ppm. Just as observed for the nonbridged molybdenocene azobenzene complex [Mo(η^5-C_5H_5)$_2$ (κ^2-PhNNPh)], the ^{1}H NMR signals of the phenyl rings are shifted upfield ($\delta = 7.36$–6.78 ppm) compared with those of free azobenzene ($\delta = 8.0$–7.2 ppm).[17] The ^{29}Si NMR shifts at $\delta = -12.9$ (**3**) and -10.7 ppm (**4**) are at the lower end of the range expected for [2]silametallocenophanes of early transition metals ($\delta = -12.7$ to -20.2 ppm).[4g,18]

Single crystals of **4** for X-ray diffraction analysis were obtained from a toluene solution at −30 °C. Complex **4** crystallizes in the monoclinic space group $P2_1/n$. Most structural parameters are in the expected range, such as the Si–Si distance of 2.3370(7) Å (2.3394(8) to 2.352(2) Å)[4g,21a] or the N–N distance of 1.4061(19) Å (1.37 to 1.43 Å)[19] (Figure 4). The coordination mode for η^2-bound azobenzene strongly depends on the nature of the central metal. In early transition metal complexes, Ph–N=N–Ph acts as a π donor and, therefore, is described as a formally dianionic ligand. However, in late transition metal complexes, it behaves as a π accepting, neutral ligand. Experimental and computational studies revealed that these differences in the electronic properties of the ligand are associated with variation of the

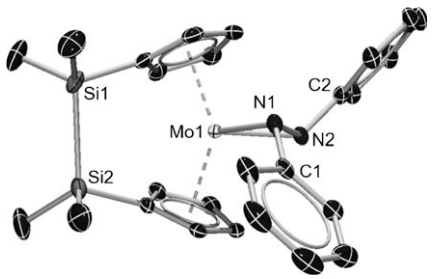

Figure 4. Molecular structure of **4**. Selected bond lengths [Å] and angles [°]: N1–N2 1.4061(9), Si1–Si2 2.3370(7), Mo1–N1 2.1144(14), Mo1–N2 2.0874(15); C1-N1-N2-C2 115.89(16).

dihedral angle between the phenyl substituents (C_{ipso}-N-N-C_{ipso}).[19] As expected for molybdenum complex **4**, the corresponding torsion angle (C1-N1-N2-C2) of 115.9° more closely resembles that of the early transition metal complex [Zr(η^5-C_5H_5)$_2$(η^2-PhNNPh)(NC_5H_5)] (91.3°) than that of the nickel species [Ni(*t*BuNC)$_2$(η^2-PhNNPh)] (153.2°).

In contrast to the aforementioned nonpolar substrates, the reaction of *tert*-butylisonitrile with **1** affords a more complex product with formal 1,2-addition of the silyl groups to the C≡N bond and coordination of the carbenoid carbon atom to the molybdenum center (Scheme 4). Monitoring the reaction by using ^{1}H NMR spectroscopy revealed almost quantitative conversion of molybdenum complex **1**. Brown carbene complex **5** is air and moisture sensitive and was isolated in 51% yield.

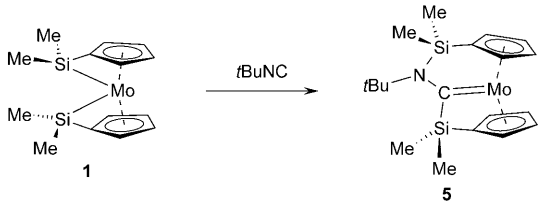

Scheme 4. Reactivity of **1** towards *tert*-butylisonitrile.

Carbene complex **5** appears C_s symmetric in solution. In the ^{1}H NMR spectrum, four signals at $\delta = 6.10$, 5.22, 4.30 and 3.86 ppm can be assigned to the cyclopentadienyl protons and two signals at $\delta = 0.42$ and 0.40 ppm to the methyl groups. The ^{13}C NMR spectrum reveals a downfield shifted signal at $\delta = 279.5$ ppm, being in the expected range for carbene complexes ([Mo(CO)$_5${C(NMe$_2$)(SiPh$_3$)}] (**6**): $\delta =$ 300.4 ppm).[20] The ^{29}Si NMR spectrum shows two signals for the silicon nuclei, one at $\delta = -4.1$ ppm for the nitrogen-bound silicon atom (R_2NSiR_3, R = alkyl, aryl: $\delta = -12.9$ to 8.2 ppm)[21] and one at $\delta = -34.8$ ppm for the carbene-bound silicon atom (**6**: $\delta = -25.6$ ppm).[22] Single crystals of **5** suitable for X-ray diffraction analysis were obtained from a solution in diethyl ether at −30 °C. Complex **5** crystallizes in the monoclinic space group $P2_1/c$. The molecular structure of **5** (Figure 5) shows a noticeably shortened Mo1−C1 distance of 2.0653(12) Å compared with those of ordinary Fischer-type molybdenum–carbene complexes ([Mo(CO)$_5$-{CMeNHP(N*i*Pr$_2$)$_2$}] (**7**): 2.204(3) Å)[23] and more resembles the Mo−C distance of the related molybdenum isonitrile complex ([Mo(η^5-C_5H_5)$_2$(CN*t*Bu)]: 1.997(4) Å).[24] Furthermore, a remarkably long N1−C1 distance of 1.4035(16) Å (**5**) for a nitrogen–carbon single bond is observed (**7**: 1.303(3) Å).[23] This bonding situation may be ascribed to molecular strain reflected by the deviation β (defined as the angle between the Si−C_{ipso} bond axes and the cyclopentadienyl ring plane) of 9.5(3)° (Si1−C_{ipso} to Cp1) and 27.6(2)° (Si2−C_{ipso} to Cp2), respectively. The overall structural description of **5** is that of a Fischer-type carbene complex in which the carbene center constitutes an integral part of an *ansa* bridge. This structural motif is highly unusual and, to the best of our knowledge, without precedence. Electronic structure analyses (Figure 6) confirm the character of a Fischer-type *ansa*-carbene complex.

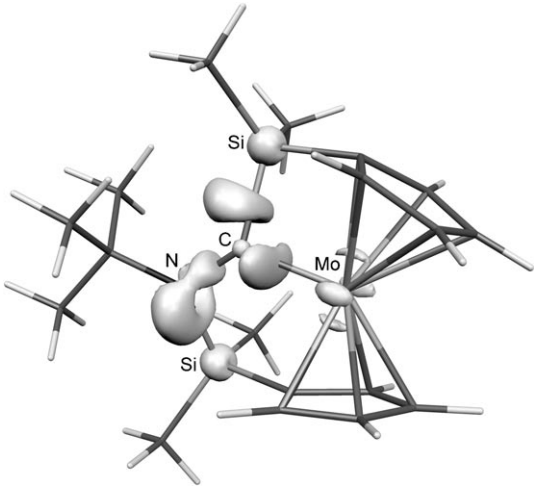

Figure 5. Molecular structure of **5**. Selected bond lengths [Å]: Mo1−C1 2.0653(12), C1−N1 1.4035(16).

Figure 6. ELF = 0.75 isosurface for $\mathbf{5}_{cs}$. ELF isosurfaces around the Cp rings, silicon methyl groups and the *t*Bu group of the CN moiety have been removed for clarity.

Conclusion

In summary, computational studies support the description of the title compound in terms of a bis-η^1:η^5-coordinated molybdenocenophane. The pronounced reactivity of **1**, as predicted on the basis of the relatively high charge at the metal center and the strained geometry, was proven in an initial series of reactions towards nonpolar and polar organic substrates. Whereas the former reactants cleanly produced [2]disilamolybdenocenophanes with side-on coordinated alkyne and diazo ligands, the polar substrate *t*Bu-N≡C gave access to a highly unusual *ansa*-carbene complex.

Experimental Section

Computational details: Wave function analyses were done for different structures of **1**. Complex $\mathbf{1}_{cs}$ is based on X-ray data[5] with only the hydrogen atom positions optimized at the BP86[25]/TZVP[26] level, with a quasi-relativistic pseudopotential for Mo.[27] The model structure $\mathbf{1}_{opt}$ was fully optimized at the B3LYP[28]/TZVP level. In the text we use subscripts to distinguish the structures of the model: "cs" refers to structures based on crystallographic data in which only the hydrogen atom positions have been optimized and "opt" refers to structures which have been fully optimized without constraints. All structure optimizations were performed with the TURBOMOLE V5.10 program package.[29] The optimized structural parameters compare well with the experimental data (see the Supporting Information). For subsequent analyses, single-point calculations on the model structure $\mathbf{1}_{cs}$ were performed at B3LYP/TZVP level by using a TZVP-based 12s6p5d all-electron basis set for Mo.[30] For all single-point calculations the Gaussian 03 program package[31] was used. NPA analyses and calculation of Wiberg bond indices for all complexes under consideration (**1**, **2**, **8**, **9**) were performed with the NBO program (version 3.1)[32] as part of the Gaussian 03 program package. NBO calculations were done both for the X-ray-based and the fully optimized structures. All values given in the text refer to the "cs" model structures. Further details and results are provided in the Supporting Information. Analysis of the electron localization function was done with a locally modified version of the TopMod program.[33] QTAIM analyses of the B3LYP/TZVP/12s6p5d electron densities of $\mathbf{1}_{cs}$ used the AIM2000 program.[34] Comparative QTAIM wave function analyses, based on BHLYP/TZVP/12s6p5d and BLYP/TZVP/12 6p5d single-point calculations, as well as analysis for the fully optimized model structure $\mathbf{1}_{opt}$, gave identical results in terms of bonding patterns.

General considerations: All manipulations were performed under an inert atmosphere of dry argon by using either standard Schlenk-line or glovebox techniques. Toluene, hexane, and diethyl ether were dried by distillation over potassium or sodium/potassium alloy. [1],[1]Disilamolybdenocenophane was synthesized according to literature procedures.[5] NMR spectra were recorded by using a Bruker Avance 500 spectrometer operating at 500.13 MHz (^{1}H, external standard TMS), 125.77 MHz (^{13}C{^{1}H}, external standard TMS), and 99.36 MHz (^{29}Si{^{1}H}, external standard TMS). Elemental analyses (C, H, N) were performed by using an Elementar Vario MICRO-cube elemental analyzer.

[Mo(Me$_2$Si)$_2$(η^5-C$_5$H$_4$)$_2$(η^2-MeCCMe)] (3): 2-butyne (0.12 mL, 1.5 mmol) was added to a solution of **1** (50 mg, 0.15 mmol) in toluene (10 mL). The reaction mixture was heated to 80 °C for 16 h. After cooling to RT, all volatile components were removed in vacuo and the crude residue was washed with hexane to give complex **3** as an orange solid (yield: 28 mg, 71 μmol, 48 %). ^{1}H NMR (C_6D_6): δ = 4.63 (virtual t, 4H, C_5H_4), 3.71 (virtual t, 4H, C_5H_4), 2.43 (s, 6H, CMe), 0.39 ppm (s, 12H, $SiMe_2$); ^{13}C{^{1}H} NMR (C_6D_6): δ = 114.6 (*C*Me), 88.9 (C_5H_4), 88.8 (C_5H_4), 85.7 (C_{ipso}, C_5H_4), 19.9 (C*Me*), −1.1 ppm ($SiMe_2$); ^{29}Si{^{1}H} NMR (C_6D_6): δ = −12.9 ppm; elemental analysis calcd (%) for $C_{18}H_{26}Si_2Mo$: C 54.80, H 6.64; found: C 53.46, H 6.56.

[Mo(Me$_2$Si)$_2$(η^5-C$_5$H$_4$)$_2$(κ^2-PhNNPh)] (4): A solution of **1** (50 mg, 0.15 mmol) in toluene (10 mL) was treated with *trans*-azobenzene (27 mg, 0.15 mmol) and the reaction mixture was heated to 80 °C for 16 h. After cooling to RT, all volatile components were removed in vacuo and the residue was recrystallized from toluene at −30 °C to give complex **4** as a red solid (yield: 40 mg, 76 μmol, 52 %). ^{1}H NMR (C_6D_6): δ = 7.36 (m, 2H, Ph), 7.27 (m, 2H, Ph), 7.13 (m, 2H, Ph), 6.84 (m, 2H, Ph), 6.78 (m, 2H, Ph), 5.09 (m, 2H, C_5H_4), 4.82 (m, 2H, C_5H_4), 4.63 (m, 2H, C_5H_4), 3.92 (m, 2H, C_5H_4), 0.17 (s, 6H, $SiMe_2$), 0.10 ppm (s, 6H, $SiMe_2$); ^{13}C{^{1}H} NMR (C_6D_6): δ = 163.7 ($C_{ipso,}$ Ph), 129.3 (Ph), 128.5 (Ph), 121.0 (Ph), 117.9 (Ph), 114.7 (Ph), 102.6 (C_5H_4), 100.8 (C_5H_4), 97.4 (C_5H_4), 97.0 (C_{ipso}, C_5H_4), 95.6 (C_5H_4), −2.0 ($SiMe_2$), −2.2 ppm ($SiMe_2$); ^{29}Si{^{1}H} NMR (C_6D_6): δ = −10.7 ppm; elemental analysis calcd (%) for $C_{26}H_{30}N_2Si_2Mo$: C 59.75, H 5.79, N 5.36; found: C 59.49, H 5.76, N 5.46.

[Mo(Me$_2$Si(*t*Bu)NCSiMe$_2$)(η^5-C$_5$H$_4$)$_2$] (5): *tert*-Butylisonitrile (20 mg, 0.24 mmol) was added to a solution of **1** (50 mg, 0.15 mmol) in toluene (10 mL) and the reaction mixture was stirred overnight. All volatile components were removed in vacuo and the residue was recrystallized from diethyl ether at −30 °C to give **5** as a brown solid (yield: 32 mg, 76 μmol, 51 %). ^{1}H NMR (C_6D_6): δ = 6.10 (virtual t, 2H, C_5H_4), 5.22 (virtual t, 2H, C_5H_4), 4.30 (virtual t, 2H, C_5H_4), 3.86 (virtual t, 2H, C_5H_4), 1.12 (s, 9H, *t*Bu), 0.42 (s, 6H, $SiMe_2$), 0.40 ppm (s, 6H, $SiMe_2$); ^{13}C{^{1}H} NMR (C_6D_6): δ = 279.5 (MoC), 90.4 (C_5H_4), 88.5 (C_{ipso}, C_5H_4), 87.4 (C_5H_4), 84.4 (C_5H_4), 80.8 (C_5H_4), 77.4 (C_{ipso}, C_5H_4), 58.7 (*C*Me$_3$), 31.8 (C*Me*$_3$), 3.1 ($SiMe_2$), 1.2 ppm ($SiMe_2$); ^{29}Si{^{1}H} NMR (C_6D_6): δ = −4.1 (SiN), −34.8 ppm (SiC); elemental analysis calcd (%) for $C_{19}H_{29}NSi_2Mo$: C 53.88, H 6.90, N 3.31; found: C 53.17, H 6.89, N 3.01.

Crystallographic analysis: The crystal data of **4** and **5** were collected by using a Bruker X8APEX diffractometer with a CCD area detector and multi-layer mirror monochromated $Mo_{K\alpha}$ radiation. The structures were solved by using direct methods, refined with the ShelX software package,[35] and expanded by using Fourier techniques. All nonhydrogen atoms were refined anisotropically. Hydrogen atoms were assigned to idealized positions and were included in structure factors calculations.

Crystal data for **4**: $C_{26}H_{30}MoN_2Si_2$; M_r = 522.64; brown block; 0.23 × 0.21 × 0.17 mm^3; monoclinic; $P2_1/n$; a = 9.9719(5), b = 16.5258(8), c = 15.8369(7) Å; α = 90.00, β = 103.163(2), γ = 90.00°; V = 2541.2(2) Å^3; Z = 4; ρ_{calcd} = 1.366 g cm^{-3}; μ = 0.626 mm^{-1}; $F(000)$ = 1080; T = 100(2) K; R_1 = 0.0341, wR_2 = 0.0950; 7315 independent reflections [$2\theta \leq 61.1°$] and 284 parameters.

Crystal data for **5**: $C_{19}H_{29}MoNSi_2$; M_r = 423.55; brown plate; 0.27 × 0.21 × 0.065 mm^3; monoclinic; $P2_1/c$; a = 14.7291(6), b = 9.2343(4), c = 14.9228(6) Å; α = 90.00, β = 103.621(2), γ = 90.00°; V = 1972.61(14) Å^3; Z = 4; ρ_{calcd} = 1.426 g cm^{-3}; μ = 0.786 mm^{-1}; $F(000)$ = 880; T = 100(2) K; R_1 = 0.0234, wR_2 = 0.0752; 5992 independent reflections [$2\theta \leq 61.02°$] and 215 parameters.

CCDC-729853 (**4**) and -729854 (**5**) contain the supplementary crystallographic data for this paper. These data can be obtained free of charge from The Cambridge Crystallographic Data Centre via www.ccdc.cam.ac.uk/data_request/cif.

Acknowledgements

This work was supported by the DFG.

[1] a) D. E. Herbert, U. F. J. Mayer, I. Manners, *Angew. Chem.* **2007**, *119*, 5152–5173; *Angew. Chem. Int. Ed.* **2007**, *46*, 5060–5081; b) V. Bellas, M. Rehahn, *Angew. Chem.* **2007**, *119*, 5174–5197; *Angew. Chem. Int. Ed.* **2007**, *46*, 5082–5104; c) P. Nguyen, P. Gomez-Elipe, I. Manners, *Chem. Rev.* **1999**, *99*, 1515–1548; d) I. Manners, *Chem. Commun.* **1999**, 857–865; e) I. Manners, *Polyhedron* **1996**, *15*, 4311–4329; f) H. G. Alt, A. Koeppl, *Chem. Rev.* **2000**, *100*, 1205–1221; g) P. C. Moehring, N. J. Coville, *Coord. Chem. Rev.* **2006**, *250*, 18–35; h) H. G. Alt, E. Samuel, *Chem. Soc. Rev.* **1998**, *27*, 323–329.

[2] a) M. Bochmann, *J. Chem. Soc. Dalton Trans.* **1996**, 255–270; b) D. E. Herbert, M. Tanabe, S. C. Bourke, A. J. Lough, I. Manners, *J. Am. Chem. Soc.* **2008**, *130*, 4166–4176.

[3] A. Bartole-Scott, H. Braunschweig, T. Kupfer, M. Lutz, I. Manners, T. L. Nguyen, K. Radacki, F. Seeler, *Chem. Eur. J.* **2006**, *12*, 1266–1273.

[4] a) W. Finckh, B. Z. Tang, A. Lough, I. Manners, *Organometallics* **1992**, *11*, 2904–2911; b) M. Herberhold, U. Steffl, W. Milius, B. Wrackmeyer, *Angew. Chem.* **1997**, *109*, 1545–1546; *Angew. Chem. Int. Ed. Engl.* **1997**, *36*, 1508–1510; c) M. Herberhold, U. Steffl, B. Wrackmeyer, *J. Organomet. Chem.* **1999**, *577*, 76–81; d) H. Braunschweig, M. Lutz, K. Radacki, *Angew. Chem.* **2005**, *117*, 5792–5796; *Angew. Chem. Int. Ed.* **2005**, *44*, 5647–5651; e) H. Braunschweig, T. Kupfer, M. Lutz, K. Radacki, F. Seeler, R. Sigritz, *Angew. Chem.* **2006**, *118*, 8217–8220; *Angew. Chem. Int. Ed.* **2006**, *45*, 8048–8051; f) H. Braunschweig, M. Lutz, K. Radacki, A. Schaumloeffel, F. Seeler, C. Unkelbach, *Organometallics* **2006**, *25*, 4433–4435; g) H. Braunschweig, T. Kupfer, *Organometallics* **2007**, *26*, 4634–4638;

h) H. Braunschweig, T. Kupfer, *J. Am. Chem. Soc.* **2008**, *130*, 4242–4243; i) H. Braunschweig, M. Kaupp, C. J. Adams, T. Kupfer, K. Radacki, S. Schinzel, *J. Am. Chem. Soc.* **2008**, *130*, 11376–11393.
[5] H. Braunschweig, M. Gross, K. Radacki, C. Rothgaengel, *Angew. Chem.* **2008**, *120*, 10127–10129; *Angew. Chem. Int. Ed.* **2008**, *47*, 9979–9981.
[6] a) R. Koch, E. Boelter, J. Stroot, R. Beckhaus, *J. Organomet. Chem.* **2006**, *691*, 4539–4544; b) J. A. Bandy, V. S. B. Mtetwa, K. Prout, J. C. Green, C. E. Davies, M. L. H. Green, N. J. Hazel, A. Izquierdo, J. J. Martin-Polo, *J. Chem. Soc. Dalton Trans.* **1985**, 2037–2049.
[7] a) A. D. Becke, K. E. Edgecombe, *J. Chem. Phys.* **1990**, *92*, 5397–5403; b) A. Savin, R. Nesper, S. Wengert, T. F. Fässler, *Angew. Chem.* **1997**, *109*, 1892–1918; *Angew. Chem. Int. Ed. Engl.* **1997**, *36*, 1808–1832.
[8] A. E. Reed, R. B. Weinstock, F. Weinhold, *J. Chem. Phys.* **1985**, *83*, 735–746.
[9] R. W. F. Bader, *Atoms in Molecules: A Quantum Theory*, Oxford University Press, Oxford, **1990**.
[10] a) J. W. Lauher, R. Hoffmann, *J. Am. Chem. Soc.* **1976**, *98*, 1729–1742; b) J. C. Green, *Chem. Soc. Rev.* **1998**, *27*, 263–271.
[11] K. B. Wiberg, *Tetrahedron* **1968**, *24*, 1083–1096.
[12] a) K. Götz, M. Kaupp, H. Braunschweig, D. Stalke, *Chem. Eur. J.* **2009**, *15*, 623–632; b) Comparative QTAIM wave function analyses based on BHLYP/TZVP/12s6p5d and BLYP/TZVP/12s6p5d single-point calculations.
[13] T. S. Koloski, D. C. Pestana, P. J. Carroll, D. H. Berry, *Organometallics* **1994**, *13*, 489–499.
[14] For example, see: A. E. Reed, L. A. Curtiss, F. Weinhold, *Chem. Rev.* **1988**, *88*, 899–926.
[15] For example, see: P. Rademacher, *Eur. J. Org. Chem.* **2004**, 1572–1576.
[16] G. E. Herberich, U. Englert, W. Fassbender, *J. Organomet. Chem.* **1991**, *420*, 303–314.
[17] A. Nakamura, M. Aotake, S. Otsuka, *J. Am. Chem. Soc.* **1974**, *96*, 3456–3462.
[18] a) K.-H. Thiele, C. Schliessburg, K. Baumeister, K. Hassler, *Z. Anorg. Allg. Chem.* **1996**, *622*, 1806–1810; b) H. Braunschweig, N. Buggisch, U. Englert, M. Homberger, T. Kupfer, D. Leusser, M. Lutz, K. Radacki, *J. Am. Chem. Soc.* **2007**, *129*, 4840–4846.
[19] M. Retboell, K. A. Joergensen, *Inorg. Chem.* **1994**, *33*, 6403–6405.
[20] E. O. Fischer, H. Hollfelder, P. Friedrich, F. R. Kreissl, G. Huttner, *Chem. Ber.* **1977**, *110*, 3467–3480.
[21] M. L. Filleux-Blanchard, D. A. Nguyen, *Org. Magn. Reson.* **1979**, *12*, 12–16.
[22] F. H. Koehler, H. Hollfelder, E. O. Fischer, *J. Organomet. Chem.* **1979**, *168*, 53–60.
[23] K. H. Dötz, F. Kroll, K. Harms, *J. Organomet. Chem.* **1993**, *459*, 169–176.
[24] A. M. Martins, M. J. Calhorda, C. C. Romao, C. Voelkl, P. Kiprof, C. Filippou, *J. Organomet. Chem.* **1992**, *423*, 367–390.
[25] a) A. D. Becke, *Phys. Rev. A* **1988**, *38*, 3098–3100; b) J. P. Perdew, *Phys. Rev. B* **1986**, *33*, 8822–8824.
[26] F. Weigend, R. Ahlrichs, *Phys. Chem. Chem. Phys.* **2005**, *7*, 3297–3305.
[27] D. Andrae, U. Haeussermann, M. Dolg, H. Stoll, H. Preuss, *Theor. Chim. Acta* **1990**, *77*, 123–141.
[28] a) A. D. Becke, *J. Chem. Phys.* **1993**, *98*, 5648–5652; b) C. Lee, W. Yang, R. G. Parr, *Phys. Rev. B* **1988**, *37*, 785–789.
[29] a) R. Ahlrichs, M. Bär, M. Häser, H. Horn, C. Kölmel, *Chem. Phys. Lett.* **1989**, *162*, 165–169; b) TURBOMOLE V5.10; http://www.turbomole.com.
[30] J. Fritscher, P. Hrobárik, M. Kaupp, *J. Phys. Chem. B* **2007**, *111*, 4616–4629.
[31] Gaussian 03, Revision B04, M. J. Frisch, G. W. Trucks, H. B. Schlegel, G. E. Scuseria, M. A. Robb, J. R. Cheeseman, J. A. Montgomery, Jr., T. Vreven, K. N. Kudin, J. C. Burant, J. M. Millam, S. S. Iyengar, J. Tomasi, V. Barone, B. Mennucci, M. Cossi, G. Scalmani, N. Rega, G. A. Petersson, H. Nakatsuji, M. Hada, M. Ehara, K. Toyota, R. Fukuda, J. Hasegawa, M. Ishida, T. Nakajima, Y. Honda, O. Kitao, H. Nakai, M. Klene, X. Li, J. E. Knox, H. P. Hratchian, J. B. Cross, V. Bakken, C. Adamo, J. Jaramillo, R. Gomperts, R. E. Stratmann, O. Yazyev, A. J. Austin, R. Cammi, C. Pomelli, J. W. Ochterski, P. Y. Ayala, K. Morokuma, G. A. Voth, P. Salvador, J. J. Dannenberg, V. G. Zakrzewski, S. Dapprich, A. D. Daniels, M. C. Strain, O. Farkas, D. K. Malick, A. D. Rabuck, K. Raghavachari, J. B. Foresman, J. V. Ortiz, Q. Cui, A. G. Baboul, S. Clifford, J. Cioslowski, B. B. Stefanov, G. Liu, A. Liashenko, P. Piskorz, I. Komaromi, R. L. Martin, D. J. Fox, T. Keith, M. A. Al-Laham, C. Y. Peng, A. Nanayakkara, M. Challacombe, P. M. W. Gill, B. Johnson, W. Chen, M. W. Wong, C. Gonzalez, J. A. Pople, Gaussian, Inc., Wallingford CT, **2004**.
[32] E. D. Glendening, A. E. Reed, J. E. Carpenter, F. Weinhold, NBO Version 3.1.
[33] a) S. Noury, X. Krokidis, F. Fuster, B. Silvi, Paris, TopMod package, **1997**; b) S. Noury, X. Krokidis, F. Fuster, B. Silvi, *Comput. Chem.* **1999**, *23*, 597–604.
[34] a) F. Biegler-Koenig, J. Schoehnbohm, Bielefeld, Germany, **2002**; b) AIM2000 Version 2.0; http://www.aim2000.de.
[35] G. Sheldrick, *Acta Crystallogr. Sect. A* **2008**, *64*, 112–122.

Received: October 19, 2009
Published online: February 9, 2010

